SAR and QSAR in Environmental Research, 2015
Vol. 26, No. 6, 507–519, http://dx.doi.org/10.1080/1062936X.2015.1070200

Taylor & Francis
Taylor & Francis Group

Combined molecular dynamics and continuum solvent approaches (MM-PBSA/GBSA) to predict noscapinoid binding to γ-tubulin dimer

C Suri[a] and P.K Naik[a,b]*

[a]*Department of Biotechnology and Bioinformatics, Jaypee University of Information Technology, Himachal Pradesh, India;* [b]*Department of Biotechnology, Guru Ghasidas Vishwavidyalaya (A Central University), Chhattisgarh, India*

(*Received 31 March 2015; in final form 3 July 2015*)

γ-tubulin plays crucial role in the nucleation and organization of microtubules during cell division. Recent studies have also indicated its role in the regulation of microtubule dynamics at the plus end of the microtubules. Moreover, γ-tubulin has been found to be over-expressed in many cancer types, such as carcinomas of the breast and glioblastoma multiforme. These studies have led to immense interest in the identification of chemical leads that might interact with γ-tubulin and disrupt its function in order to explore γ-tubulin as potential chemotherapeutic target. Recently a colchicine-interacting cavity was identified at the interface of γ-tubulin dimer that might also interact with other similar compounds. In the same direction we theoretically investigated binding of a class of compounds, noscapinoids (noscapine and its derivatives) at the interface of the γ-tubulin dimer. Molecular interaction of noscapine and two of its derivatives, amino-noscapine and bromo-noscapine, was investigated by molecular docking, molecular dynamics simulation and binding free energy calculation. All noscapinoids displayed stable interaction throughout simulation of 25 ns. The predictive binding free energy (ΔG_{bind}) indicates that noscapinoids bind strongly with the γ-tubulin dimer. However, bromo-noscapine showed the best binding affinity (ΔG_{bind} = –37.6 kcal/mol) followed by noscapine (ΔG_{bind} = –29.85 kcal/mol) and amino-noscapine (ΔG_{bind} = –23.99 kcal/mol) using the MM-PBSA method. Similarly using the MM-GBSA method, bromo-noscapine showed highest binding affinity (ΔG_{bind} = –43.64 kcal/mol) followed by amino-noscapine (ΔG_{bind} = –37.56 kcal/mol) and noscapine (ΔG_{bind} = –34.57 kcal/mol). The results thus generate compelling evidence that these noscapinoids may hold great potential for preclinical and clinical evaluation.

Keywords: γ-tubulin; noscapine; noscapinoids; molecular docking; molecular dynamics; free energy calculation; MM-PBSA; MM-GBSA

1. Introduction

γ-tubulin is an essential component of the microtubule organization centre (MTOC). It is known to interact with the minus end of microtubules and found to be localized at the centrosome. It plays an extremely crucial role in the nucleation and organization of microtubules [1,2]. At the MTOC, γ-tubulin forms complexes with other proteins to form γ-tubulin small complex (γTuSC, around 280 kDa) that comprises two molecules of γ-tubulin and one molecule each of GCP (γ-tubulin complex protein) 2 and 3. These proteins structurally associate to form a flexible Y-shaped structure with γ-tubulins located on the two arms. Furthermore, 5–7

*Corresponding author. Email: pknaik1973@gmail.com

γTuSCs associate together to form the larger cone-shaped complex known as γ-tubulin-ring complex (γTuRC), in association with GCP4, GCP5 and GCP6 [3–9] in which γ-tubulin forms the rim. Within γTuRC, γ-tubulin interacts directly via one of its longitudinal interfaces with the minus end of microtubules and via the other longitudinal interface with the GCPs (GCP2, GCP3, GCP4). Further, the γ-tubulin interacts laterally with another γ-tubulin.

Many drugs that are currently administered as chemotherapeutic regimes, such as paclitaxel derivatives and vinca-alkaloids, bind to α/β tubulin and target mitotic spindle dynamics [10]. However, these drugs are plagued with many drawbacks, such as development of multi-drug resistance over time, which often leave patients with more aggressive tumours and side effects. Indiscriminate and prolonged use of microtubule-targeting drugs affects normal rapidly dividing cells like those of the hair follicles and intestinal lining, causing hair loss and nausea. These drawbacks call for continuous progressive research to identify newer drugs with no or negligible side effects.

In recent studies γ-tubulin has been found to be over-expressed in pre-invasive lesions, carcinomas of the breast and glioblastoma multiforme [11–14]. Since γ-tubulin over-expression is associated with tumour progression, a potent inhibitor of γ-tubulin would possibly halt mitosis in cancer cells. In the endeavour to explore if noscapine and its potential derivatives could bind at the interface and disrupt the γ-γ-tubulin lateral interactions, we studied probable binding interaction of noscapine, amino-noscapine and bromo-noscapine with the γ-tubulin homodimer. To achieve this, we first prepared the structure of the γ-tubulin homodimer and ligands. We then performed molecular docking to obtain the protein–ligand complexes, which were then simulated for 25 ns. We predicted the binding affinity between the γ-tubulin homodimer and ligands using the Molecular Mechanics/Poisson Boltzmann Surface Area (MM/PBSA) and the Molecular Mechanics/Generalized Born Surface Area (MM/GBSA). Both MM/PBSA and the MM/GBSA methods are employed to calculate binding free energies for macromolecules by combining molecular mechanics calculations and continuum solvation models. Both these methods have been widely used to calculate binding affinities [15–17].

2. Materials and methods

2.1 *Protein structure preparation*

The co-ordinates of the γ-tubulin dimer (PDB ID: 3CB2, Resolution 2.3 Å) were obtained from the Protein Data Bank. Minor errors in the crystal structure were corrected as reported previously [18]. Briefly, the 14 non-terminal missing amino acids were filled based on multiple template homology modelling using the structure of 3CB2 (Chain A), 2Q1F (Chain A) and 2D2M (Chain D) as templates. The missing side chains in the modelled structure were incorporated using Prime (version 3.0, Schrodinger) followed by MD simulation for 25 ns. An average structure was generated using the last 1500 frames from the total of 2500 frames generated every 10 ps.

2.2 *Ligand preparation*

The molecular structure of noscapine and two of its derivatives, amino-noscapine and bromo-noscapine **1–3** (Figure 1), were built by sketching the molecules and converting them to their 3D representation using molecular builder of Maestro (version 8.5, Schrodinger LLC). *In vacuo* energy minimization was performed on all the three structures by means of molecular mechanics force field (OPLS 2005) with default setting using Impact (version 5.6,

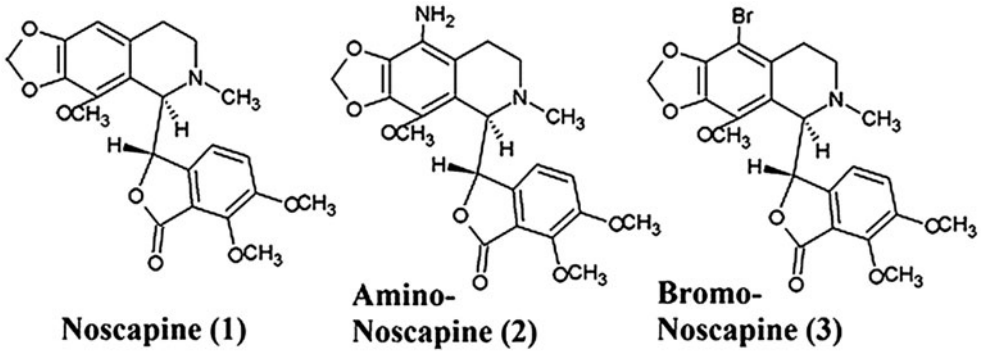

Figure 1. Molecular structure of ligands: noscapine (1), amino-noscapine (2) and bromo-noscapine (3).

Schrodinger, LLC). Appropriate bond orders were assigned to each structure using Ligprep (version 2.4, Schrodinger LLC). Ligprep is a utility tool of the Schrodinger software suite that combines tools for searching for tautomers and steric isomers and performs optimization of ligands. All the ligands were minimized with the help of the OPLS 2005 force field with default options of 32 stereo isomers, tautomers and ionization at biological pH 7±2. Furthermore, complete geometrical optimization of these ligands was performed in Jaguar (version 7.7, Schrodinger, LLC) using hybrid density functional theory with Becke's three-parameter exchange potential and the Lee–Yang–Parr correlation functional [19,20] using basis set 3-21G* level [21–23].

2.3 *Molecular docking*

After ensuring that protein and ligands were in correct form, molecular docking of the optimized ligands onto the γ-tubulin dimer was performed using Glide (version 4.5, Schrodinger, LLC). We adapted a blind docking approach, in which all the possible binding sites of the γ-tubulin dimer were predicted based on SiteMap (version 2.4, Schrodinger) [24] and used for molecular docking of ligands. SiteMap uses Goodford's grid algorithm to define a binding site with a set of site points [25]. For comparative analyses, only those binding sites which consist of at least five site points were considered. The best way to understand the noscapinoid binding site is to obtain a co-crystal structure with tubulin, which is not yet possible. The physicochemical properties of the predicted binding sites are included in Table 1. The receptor-grid file was generated using a grid receptor generation program with van der Waals scaling of 0.4 Å. A grid box size of 10 Å each for the bounding and enclosing boxes was generated at the centroid of the predicted binding sites. The ligands were docked into the binding site first using the "standard precision" method and further refined using "extra precision" Glide algorithm [22–24]. For the ligand docking stage, a scale factor of 0.4 for van der Waals radii was applied to atoms of protein with absolute partial charges less than or equal to 0.25. Out of the 10,000 poses that were sampled, 1000 were taken through minimization (conjugate gradient) and the 30 structures having the lowest energy conformations were further evaluated for a favourable Glide docking score. The binding site located at the interface of the γ-tubulin dimer with better docking score with all the ligands was selected as the putative binding site. The single best conformation for each ligand–protein complex was selected for further molecular modelling calculations.

Table 1. Prediction of different binding sites on the γ-tubulin dimer complex along with their physico-chemical properties.

Binding site	*Site score*	*Volume (Å)^3*	*Exposure*	*Enclosure*	*Contact*	*Phobic*	*Philic*	*Balance*	*Don/ Acc*
1	1.056	952.5	0.516	0.781	0.976	0.860	1.032	0.834	1.136
2	0.983	497.3	0.616	0.725	0.855	0.259	1.112	0.233	1.173
3	1.062	438.3	0.417	0.791	1.085	0.093	1.695	0.055	0.413
4	1.048	423.9	0.458	0.769	1.003	0.070	1.657	0.042	0.436
5	0.900	163.6	0.640	0.658	0.873	0.112	1.096	0.102	0.726
6	0.988	299.4	0.698	0.725	0.725	0.582	0.803	0.725	0.173
7	0.906	164.3	0.595	0.737	0.938	0.484	1.232	0.392	0.623
8	0.893	162.9	0.598	0.704	0.857	0.540	1.108	0.487	0.597
9	0.931	158.8	0.601	0.729	1.018	0.247	1.222	0.202	0.642
10	0.824	160.9	0.726	0.622	0.765	0.449	0.823	0.546	0.759

2.4 *Molecular dynamics simulation and binding affinity calculation*

The protein–ligand complexes obtained after molecular docking were then simulated for 25 ns in Amber 11. Before simulation, the missing parameters for all three ligands were estimated with the antechamber program [26] implemented in Amber 11. The AM1-BCC charge model was used to calculate the atomic point charges [27]. Missing hydrogens were added and the FF99SB forcefield was employed to assigned parameters to the complex of GCP4 and γ-tubulin, while the GAFF forcefield was used to assigned the parameters to each ligand using tleap module available in Amber 11. Each system was neutralized using sodium ions and solvated using TIP3 water model in a truncated octahedron with distance of at least 15 Å between the wall of the box and the closest atom of the complex [28].

Each protein–ligand system was subjected to three consecutive rounds of energy minimization to relax the molecular system and to remove bad contacts, using a time step of 2 fs for 2000 steps. Positions restraints of 10 kcal^{-1}Å^{-2} and 2 kcal^{-1}Å^{-2} were imposed on the protein system for the first and the second rounds, respectively, to allow relaxation of solvent molecules. No restraints were imposed in the third round. The minimized systems were gradually heated from 0 to 300 K. The molecular systems were then equilibrated for 500 ps at 300 K and 1 atm pressure. After all the thermodynamic properties were stabilized, the molecular system was simulated for 25 ns with a time step of 2fs. Throughout the simulation, temperature was regulated using the Langevin thermostat. The electrostatic interactions were calculated using the Particle Mesh Ewald [29,30] method, while the bonds were constrained using the Shake algorithm [31]. The non-bonded cut-off distance was kept at 10 Å. Co-ordinates were written to the trajectory file every 10 ps. A total of 2500 frames were obtained after 25 ns simulation. All trajectories were analysed using the PTRAJ program implemented in Ambertools [32].

Binding affinity of noscapinoids at the γ-γ-tubulin binding interface was then calculated using MM-PBSA and MM-GBSA methods [15,33]. Free energy of binding was calculated as the ensemble average of the binding free energy of a total of 1500 snapshots, extracted every 10 ps from the last 15 ns of the MD simulation trajectory.

$$\Delta G_{\text{bind}} = \Delta G_{\text{complex}} - [\Delta G_{\text{Rec}} + \Delta G_{\text{lig}}]$$
$$G = E_{\text{gas}} + G_{\text{sol}} - TS.$$
$$E_{\text{gas}} = E_{\text{int}} + E_{\text{ele}} + E_{\text{vdw}}$$
$$G_{\text{sol}} = G_{\text{PB(GB)}} + G_{\text{sol-np}}$$
$$G_{\text{sol-np}} = \gamma SAS$$

Table 2. Molecular docking evaluation of binding sites. All three ligands were docked onto the 10 predicted binding sites of the γ-tubulin dimer complex. The binding site that showed better docking score with all the ligands was selected as the probable binding site of interaction of these ligands on the γ-γ tubulin dimer. On the basis of docking score, site 6 was selected.

Ligand	*Site 1*	*Site 2*	*Site 3*	*Site 4*	*Site 5*	*Site 6*	*Site 7*	*Site 8*	*Site 9*	*Site 10*
Amino	-2.81	-2.9	-3.48	-3.36	-3.1	**-3.55**	-1.88	-2.54	-3.08	-2.61
Bromo	-2.54	-2.94	-3.09	-2.7	-2.42	**-4.23**	-1.66	-2.48	-2.36	-2.82
Noscapine	-1.63	-2.26	-1.91	-1.97	-1.84	**-2.67**	-1.74	-2.14	-1.93	-1.88

where ΔG_{bind} represents the binding free energy between receptor and ligand and is calculated as the difference between the binding free energy of the complex ($\Delta G_{complex}$) and the sum of the binding free energy of receptor (ΔG_{Rec}) and ligand (ΔG_{lig}). *G* is Gibbs free energy, *TS* is the comformational entropy, E_{gas} is the gas phase energy calculated as the sum of internal energy (E_{int}), energy generated as a result of the electrostatic interaction (E_{ele}) and the van der Waals interaction (E_{vdw}). G_{sol} is the solvation free energy calculated as the sum of polar ($G_{PB(GB)}$) and non-polar contributions ($G_{sol\text{-}np}$). Polar interaction contribution ($G_{ELE,PB(GB)}$) was calculated as the summation of electrostatic contribution (E_{ele}) and polar solvation contribution ($G_{PB(GB)}$). The non-polar solvation contribution ($G_{sol\text{-}np}$) is approximated as

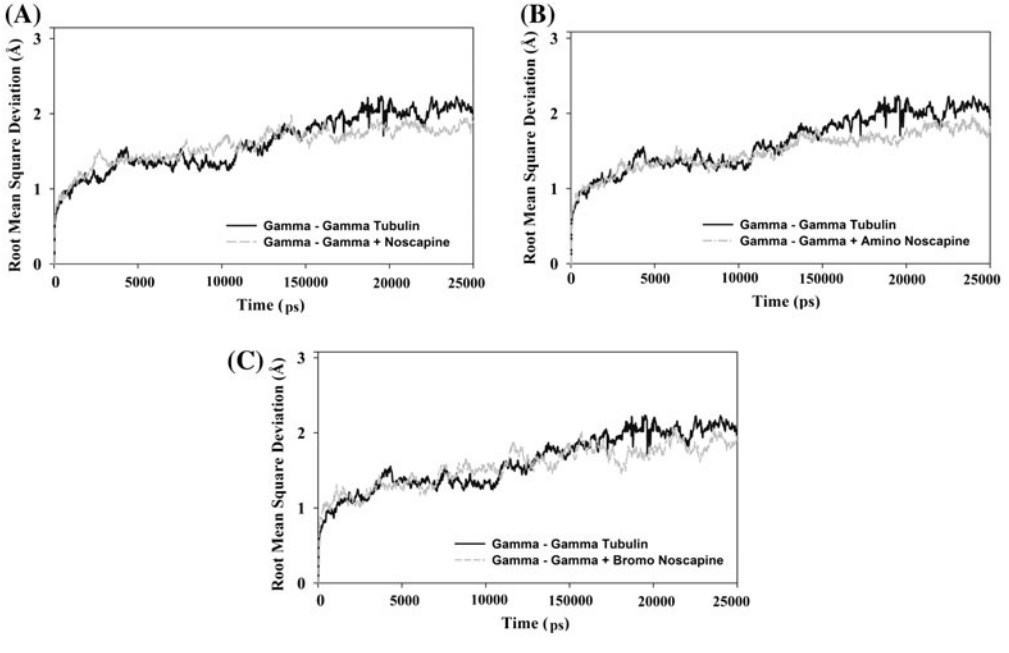

Figure 2. Root mean square deviation. The root mean square deviation (RMSD) of Cα atoms of the γ-tubulin dimer in the free form and bound form with different ligands – (A) noscapine, (B) amino-noscapine and (C) bromo-noscapine – during the entire duration of MD simulation. All molecular systems display stability throughout 25 ns simulation.

linearly dependent on the solvent accessible surface area (*SAS*) and γ is the surface tension constant that was set to 0.0072 kcal mol^{-1} $Å^{-2}$ [33].

2.5 *Per-residue energy decomposition*

The contribution of each amino acid residue of the γ-tubulin dimer was calculated to identify those residues which show strong interaction with noscapinoids. These calculations were performed using MM-GBSA method implemented in Amber 11 over 1500 frames obtained every 10 ps from last 15 ns trajectory. The residues that contributed more than –1 kcal/mol to the stability of the protein–ligand complex were designated as hot-spot amino acids. The energy contribution of each amino acid was further decomposed into various energy components such as van der Waals, electrostatic, polar solvation and non-polar solvation energy components.

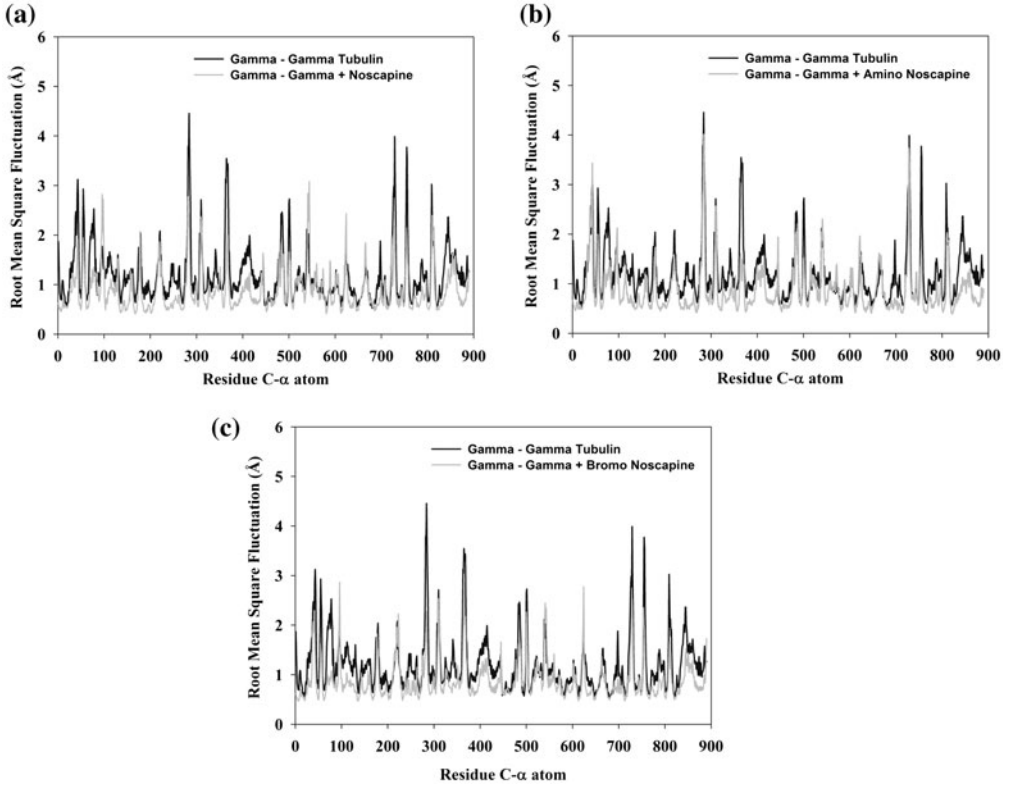

Figure 3. Root mean square fluctuation (RMSF) of Cα atoms. RMSF of residues in the γ-tubulin dimer in the free form and in the bound form with different ligands – (A) noscapine, (B) amino-noscapine, (C) bromo-noscapine – during the entire duration of MD simulation. The residues with higher RMSF tend to show more flexibility. The residues in the bound form show a small degree of flexibility when compared with free γ-tubulin dimer.

3. Results and discussion

3.1 *Binding of noscapinoids with γ-tubulin dimer*

The molecular interaction and binding affinity of noscapinoids with the γ-tubulin dimer was determined using a combination of molecular docking, molecular dynamics simulation and MM-PBSA/MM-GBSA calculations. A blind docking approach was employed whereby noscapinoids were docked into each one of the predicted binding sites of the γ-tubulin dimer. The probable binding site of noscapinoids was then screened out based on better docking score – the binding site 6 that showed better docking score with noscapinoids was selected (Table 2). The γ-tubulin dimer complex bound to drugs (**1**–**3**) was simulated for 25 ns to obtain a trajectory of 2500 frames, each frame recorded every 10 ps. Root mean square deviations (RMSD) of Cα-atoms during the entire duration of simulation were calculated for all the frames to monitored the stability of the system. The molecular systems were observed to be stabilized after 5 ns of simulation (Figure 2), since the relative fluctuation in the RMSD of Cα carbon atoms (Cα-rmsd) was very small after equilibration. The overall RMSD ranges from 0 to 2.2 Å. Furthermore, root mean square fluctuations (RMSF) of Cα-atoms of the molecular systems were calculated to find any changes in the residue flexibilities. The RMSF values were plotted against residue numbers as shown in Figure 3. The residues with higher

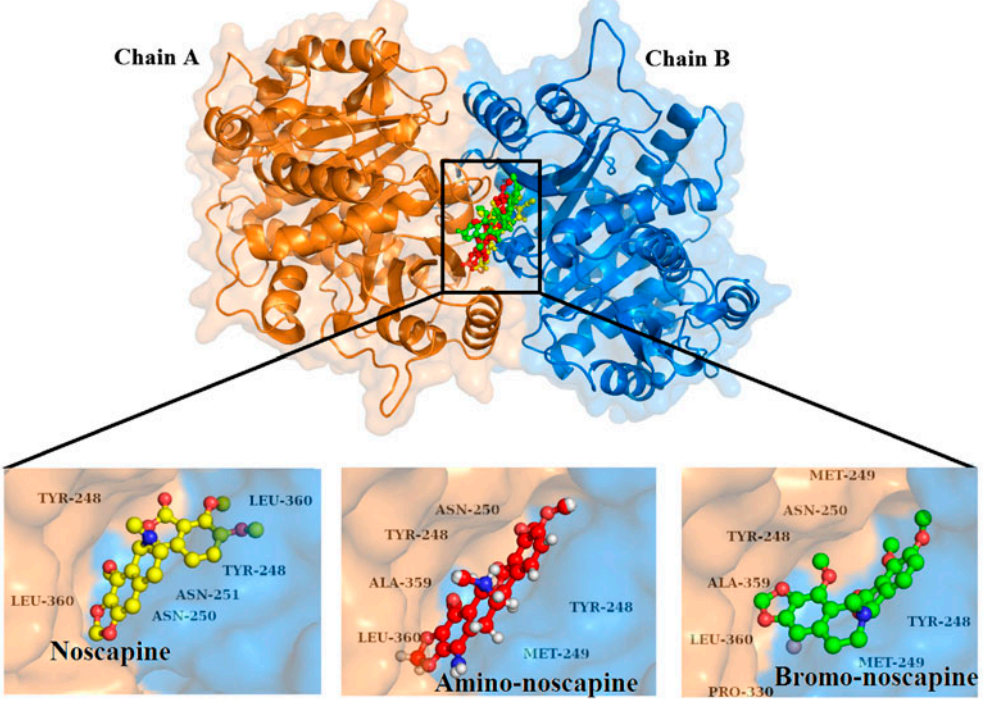

Figure 4. Binding mode of noscapinoids. Noscapinoids (noscapine, amino-noscapine and bromo-noscapine) docked into the γ-tubulin dimer. The zoomed views show the binding mode of the noscapinoids alone. The residues which show contribution of less than –1 kcal/mol to the binding free energy (ΔG_{bind}) are only labelled.

RMSF tended to show more flexibility (Figure 3). The binding modes of noscapinoids were found to involve interactions with both γ-tubulin units at the interface region and are well accomodated inside the binding cavity (Figure 4).

3.2 *Theoretical binding affinity calculation*

The binding affinity of all the three noscapinoids (1–3) was calculated using MM-PBSA and MM-GBSA methods. All three noscapinoids displayed stable interaction throughout simulations (Figures 3 and 4). Among the three noscapinoids, bromo-noscapine showed the best binding affinity with the value of –37.6 kcal/mol, followed by noscapine with –29.85 kcal/mol and amino-noscapine with –23.99 kcal/mol using the MM-PBSA method (Table 3). Using the MM-GBSA method, bromo-noscapine showed highest binding affinity with the value of –43.64 kcal/mol, followed by amino-noscapine with –37.56 kcal/mol and noscapine with the value of –34.57 kcal/mol. This could be attributed to the formation of hydrogen bonds between bromo-noscapine and surrounding amino acid residues such as Met249, Asn250 and Gly247 in chain A (Figure 5). Noscapine also forms hydrogen bonds with Met249 and Ans250 of chain B. No significant hydrogen bonding was observed for amino-noscapine.

For all complexes, the binding energy was decomposed into its various energy components (the electrostatic, van der Waals and solvation). Both van der Waals (ΔE_{VDW}) and the electrostatic component (ΔE_{ELE}) were observed to make very significant contributions to the free energy of binding (Table 3). However, the net polar contribution ($\Delta G_{(ele,PB/GB)} = \Delta E_{ele} + \Delta G_{(PB/GB)}$) was rendered unfavourable due to very large penalty imposed by the desolvation component ($\Delta G_{PB/GB}$), while the net non-polar components ΔE_{vdw} and $\Delta G_{sol\text{-}np}$ were observed to make highly favourable contributions to the binding free energy (Figure 6).

Table 3. Calculated binding free energy using MM-GBSA and MM-PBSA to ascertain the strength of interaction between noscapinids and the γ-tubulin dimer. The major energy components such as van der Waals, electrostatic, polar solvation and non-polar solvation, contributing to the binding free energy were also estimated.

Contribution	*Noscapine (kcal/mol)*	*Amino-noscapine (kcal/mol)*	*Bromo-noscapine (kcal/mol)*
ΔE_{INT}	0.00	0.00	0.00
ΔE_{VDW}	-47.74	-54.15	-55.17
ΔE_{ELE}	-121.68	-108.00	-139.56
$\Delta E_{GAS/\ \Delta E\ MM}$	-169.41	-162.14	-194.72
ΔG_{PB}	142.84	141.70	160.60
$\Delta G_{SOL\text{-}NP}$	-3.28	-3.55	-3.48
$\Delta G_{SOLV,PB}$	139.56	138.15	157.12
$\Delta G_{ELE,PB}$	17.89	30.15	17.56
$H_{TOT,PB}$	**-29.85**	**-23.99**	**-37.60**
G_{GB}	139.59	129.89	156.21
$G_{SOLV,GB}$	134.84	124.58	151.08
$G_{ELE\ GB}$	17.91	21.89	16.65
$H_{TOT,\ GB}$	**-34.57**	**-37.56**	**-43.64**

ΔE_{INT} is internal energy, ΔE_{VDW} is energy generated due van der Waal's forces, ΔE_{ELE} is energy generated due electrostatic forces, $\Delta E_{GAS/\ \Delta E\ MM}$ is the molecular mechanics energy, $\Delta G_{SOL\text{-}NP}$ is the non-polar solvation energy, $G_{PB(GB)}$ is the polar solvation energy, $\Delta G_{SOLV,PB(GB)}$ is the total solvation energy, $\Delta G_{ELE,PB(GB)}$, Polar interaction contribution ($G_{ELEPB(GB)}$) was calculated as the summation of electrostatic contribution (E_{ele}) and polar solvation contribution ($G_{PB(GB)}$). $H_{TOT,PB(GB)}$ is the binding free energy. PB refers to values obtained using MM-PBSA method and GB refers to values obtained using MM-GBSA method.

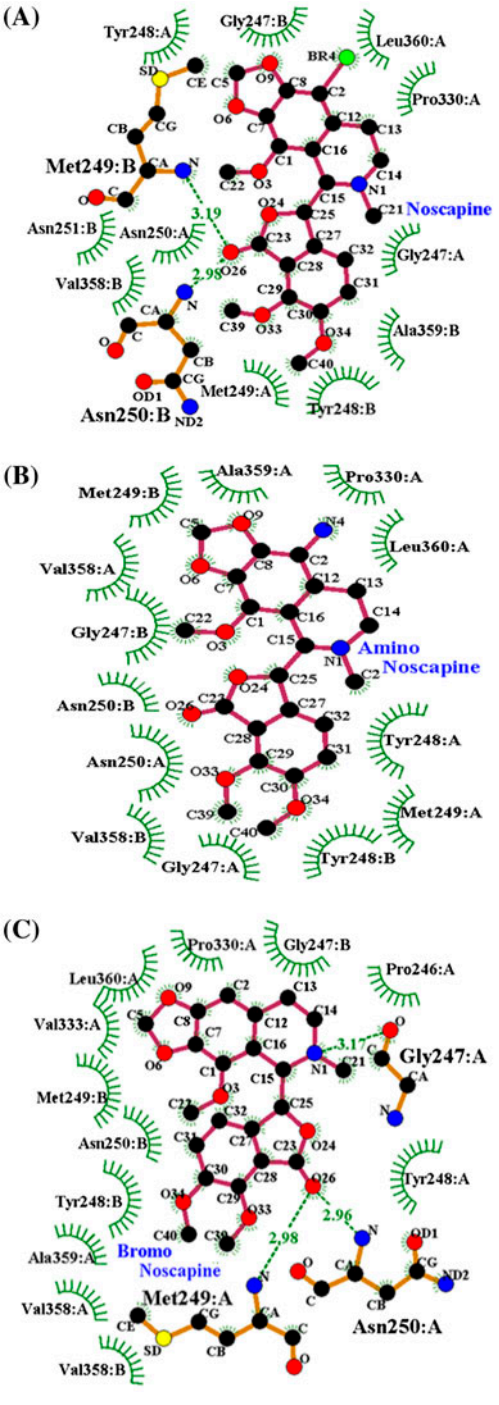

Figure 5. 2D ligplot of noscapinoids: A 2D representation of the binding mode of noscapinoids – (A) noscapine, (B) amino-noscapine and (C) bromo-noscapine – with the γ-tubulin dimer. 'A' and 'B' denote the chains in γ-tubulin dimer. Hydrogen bonding residues are shown in green and red for chain A and chain B, respectively. The dashed lines denote hydrogen bonds and numbers indicate the length of hydrogen bond. Hydrophobic interactions are shown as arcs with radial spokes. An average structure generated from last 1500 frames was used for the analysis. The figures were made using Dimplot [34].

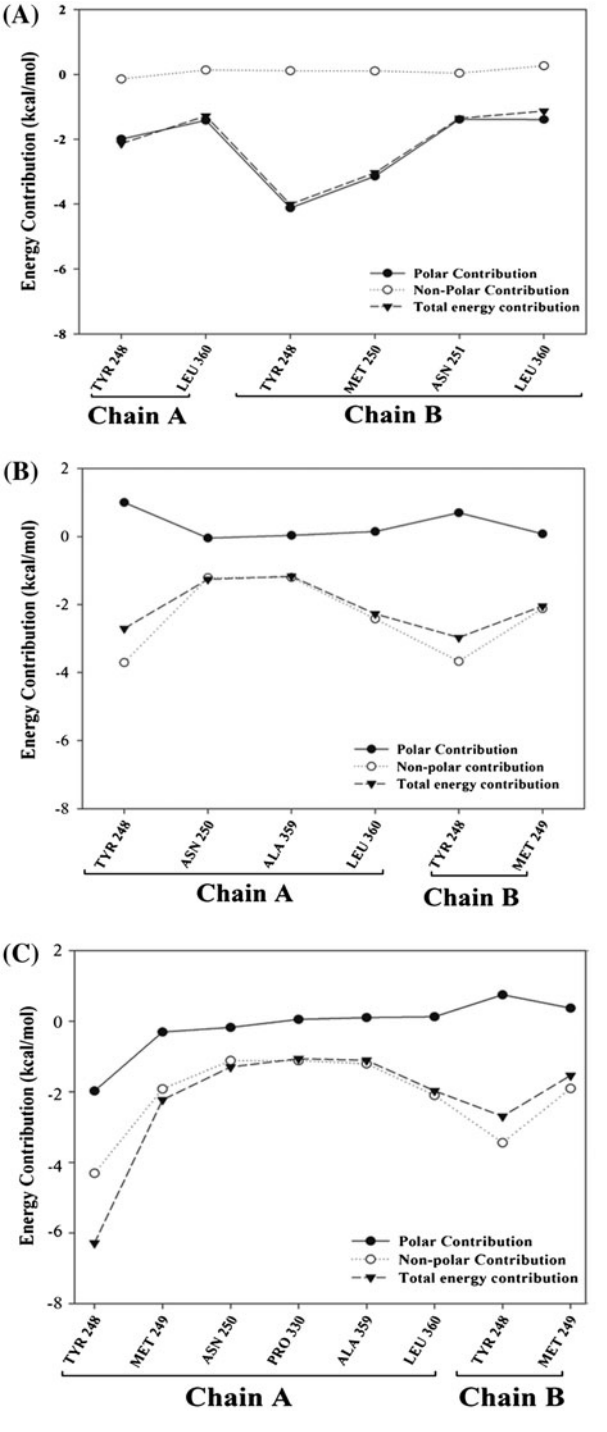

Figure 6. Energy contribution of hot-spot amino acids. Non-polar, polar as well as total energy contributions of the amino acid residues that contribute most to the stability of the protein–ligand (A) noscapine, (B) amino-noscapine and (C) Bromo-noscapine complex. Polar interactions were calculated as sum of electrostatic ($\Delta E_{i,ele}$) and polar solvation ($\Delta G_{i,sol,GB}$) energy components while the non-polar interactions were calculated as sum of van der Waals ($\Delta E_{i,vdw}$) and non-polar solvation component ($\Delta G_{i,sol\text{-}np}$).

Table 4. Energy decomposition. Decomposition of calculated $\Delta G_{bind,GB}$ (kcal/mol) on per-residue basis into total polar and non-polar energy components for the hot-spot amino acids. Those amino acids which contributed more than –1 kcal/mol to the binding affinity of noscapinoids with the γ-tubulin dimer complex were considered as hot-spot amino acids.

	γ-tubulin chain	*Residue*	*Polar contribution*	*Non-polar contribution*	*Total*
Noscapine	A	TYR 248	-1.977	-4.309	-6.287
		MET 249	-0.309	-1.922	-2.231
		ASN 250	-0.179	-1.12	-1.299
		PRO 330	0.051	-1.118	-1.067
		ALA 359	0.1	-1.209	-1.109
		LEU 360	0.126	-2.102	-1.976
	B	TYR 248	0.746	-3.444	-2.698
		MET 249	0.368	-1.909	-1.54
Amino-noscapine	A	TYR 248	0.999	-3.708	-2.71
		ASN 250	-0.046	-1.212	-1.257
		ALA 359	0.032	-1.201	-1.17
		LEU 360	0.146	-2.425	-2.279
	B	TYR 248	0.697	-3.672	-2.975
		MET 249	0.076	-2.124	-2.047
Bromo-noscapine	A	TYR 248	-1.998	-0.142	-2.14
		LEU 360	-1.423	0.135	-1.287
	B	TYR 248	-4.12	0.109	-4.012
		MET 249	-3.143	0.105	-3.038
		ASN 250	-1.391	0.035	-1.356
		LEU 360	-1.395	0.264	-1.131

Per-residue energy decomposition analysis was performed for all three complexes where the energy contribution of each residue in the complex was calculated. The residues which contributed more than –1 kcal/mol were identified as hot-spot amino acids. A total of eight hot-spot amino acids were identified for the complex of γ-tubulin dimer and noscapine, while six hot-spot amino acids were identified for complex of γ-tubulin dimer and amino-noscapine as well as the γ-tubulin dimer–bromo-noscapine complex (Table 4). The energy contribution of all the hot-spot amino acids was further decomposed into energy components such as van der Waals, electrostatic, polar solvation and non-polar solvation energy. Total polar contribution was estimated as summation of electrostatic and polar solvation energy components, while the total non-polar contribution was estimated as summation of van der Waals and non-polar solvation energy components. Further analysis revealed that Tyr 248 and Met 249 in both chains of the γ-tubulin dimer contributed significantly to the binding (Table 4) and thus play a crucial role in the binding of noscapinoid with γ-tubulin.

4. Conclusion

In this study, the binding modes of the three noscapinoids – noscapine, amino-noscapine and bromo-noscapine – with the γ-γ-tubulin dimer were illustrated using molecular dynamics simulations and continuum solvent (MM-GBSA/PBSA) approaches. It was revealed that all three noscapinoids bind to the γ-tubulin dimer in a pocket located at the binding interface between two adjacent γ-tubulin units. These results provide the first evidence of the possibility of binding of noscapinoids with γ-γ-tubulin dimer. Further work is still required to experimentally confirm the binding location of these compounds to γ-γ-tubulin dimer, so that focused

virtual screening and design of new derivatives can be undertaken to find a highly selective and specific inhibitor of the γ-γ-tubulin dimer based on the scaffold structure of noscapinoids. Such an inhibitor may eventually yield therapeutic benefit in cancer treatment. It is well proven that noscapinoids bind at the interface of α- and β-tubulin stoichiometrically and perturb microtubule dynamics just enough to induce apoptosis to cancer cells without affecting normal cells. The findings in this study might also explain an additional mode of action of these compounds, namely their possible inhibition of the γ-γ-tubulin dimer. Further study is required to determine whether noscapinoids destabilize the γTuRC, which is employed to nucleate microtubules.

Disclosure statement

No potential conflict of interest was reported by the authors.

References

[1] H.C. Joshi, M.J. Palacios, L. McNamara, and D.W. Cleveland, *γ-Tubulin is a centrosomal protein required for cell cycle-dependent microtubule nucleation*, Nature 365 (1992), pp. 80–83.

[2] B.R. Oakley, C.E. Oakley, Y. Yoon, and M.K. Jung, *γ-Tubulin is a component of the spindle pole body that is essential for microtubule function in* Aspergillus nidulans, Cell 61 (1990), pp. 1289–1301.

[3] V.R. Guillet, M. Knibiehler, and L. Gregory-Pauron, M.H.l.N. Remy, C.C. Chemin, B. Raynaud-Messina, C.c. Bon, J.M. Kollman, D.A. Agard, and A. Merdes, *Crystal structure of γ-tubulin complex protein GCP4 provides insight into microtubule nucleation*, Nat. Struct. Mol. Biol. 18 (2011), pp. 915–919.

[4] T. Horio, S. Uzawa, M.K. Jung, B.R. Oakley, K. Tanaka, and M. Yanagida, *The fission yeast gamma-tubulin is essential for mitosis and is localized at microtubule organizing centers*, J. Cell Sci. 99 (1991), pp. 693–700.

[5] H.C. Joshi, *γ-Tubulin: The hub of cellular microtubule assemblies*, BioEssays 15 (1993), pp. 637–643.

[6] J.M. Kollman, A. Zelter, E.G.D. Muller, B. Fox, L.M. Rice, T.N. Davis, and D.A. Agard, *The structure of the γ-tubulin small complex: Implications of its architecture and flexibility for microtubule nucleation*, Mol. Biol. Cell 19 (2008), pp. 207–215.

[7] K. Oegema, C. Wiese, O.C. Martin, R.A. Milligan, A. Iwamatsu, T.J. Mitchison, and Y. Zheng, *Characterization of two related* Drosophila *γ-tubulin complexes that differ in their ability to nucleate microtubules*, J. Cell Biol. 144 (1999), pp. 721–733.

[8] Y. Zheng, M.K. Jung, and B.R. Oakley, *γ-Tubulin is present in* Drosophila melanogaster *and* Homo sapiens *and is associated with the centrosome*, Cell 65 (1991), pp. 817–823.

[9] J. Zhou and P. Giannakakou, *Targeting microtubules for cancer chemotherapy*, Curr. Med. Chem. Anti-Cancer Agents 5 (2005), pp. 65–71.

[10] C. Dumontet and M.A. Jordan, *Microtubule-binding agents: A dynamic field of cancer therapeutics*, Nat. Rev. Drug Discov. 9 (2010), pp. 790–803.

[11] C.D. Katsetos, E. Dráberová, B. Smejkalova, G. Reddy, L. Bertrand, J.P. de Chadaravian, A. Legido, J. Nissanov, P.W. Baas, and P. Dráber, *Class III β-tubulin and γ-tubulin are co-expressed and form complexes in human glioblastoma cells*, Neurochem. Res. 32 (2007), pp. 1387–1398.

[12] C.D. Katsetos, E. Dráberová, A. Legido, and P. Dráber, *Tubulin targets in the pathobiology and therapy of glioblastoma multiforme. II. γ-tubulin*, J. Cell. Physiol. 221 (2009), pp. 514–520.

[13] C.D. Katsetos, G. Reddy, E. Dráberová, B. Smejkalova, L. Del Valle, Q. Ashraf, A. Tadevosyan, K. Yelin, T. Maraziotis, and O.P. Mishra, *Altered cellular distribution and subcellular sorting of γ-tubulin in diffuse astrocytic gliomas and human glioblastoma cell lines*, J. Neuropathol. Exp. Neurol. 65 (2006), pp. 465–477.

[14] L.T. Niu Y, G.M. Tse, B. Sun, R. Niu, H.M. Li, H. Wang, Y. Yang, X. Ye, Y. Wang, Q. Yu, and F. Zhang, *Increased expression of centrosomal a, g-tubulin in atypical ductal hyperplasia and carcinoma of the breast*, Cancer Sci. 100 (2009), pp. 580–587.
[15] P.A. Kollman, I. Massova, C. Reyes, B. Kuhn, S. Huo, L. Chong, M. Lee, T. Lee, Y. Duan, and W. Wang, *Calculating structures and free energies of complex molecules: Combining molecular mechanics and continuum models*, Acc. Chem. Res. 33 (2000), pp. 889–897.
[16] J. Wang, T. Hou, and X. Xu, *Recent advances in free energy calculations with a combination of molecular mechanics and continuum models*, Curr. Comput. Aided Drug Des. 2 (2006), pp. 287–306.
[17] W. Wang, O. Donini, C.M. Reyes, and P.A. Kollman, *Biomolecular simulations: Recent developments in force fields, simulations of enzyme catalysis, protein-ligand, protein-protein, and protein-nucleic acid noncovalent interactions*, Annu. Rev. Bioph. Biom. 30 (2001), pp. 211–243.
[18] C. Suri, T.W. Hendrickson, H.C. Joshi, and P.K. Naik, *Molecular insight into γ-γ tubulin lateral interactions within the γ-tubulin ring complex (γ-TuRC)*, J. Comput. Aided Mol. Des. 28 (2014), pp. 961–972.
[19] A.D. Becke, *A new mixing of Hartree-Fock and local density functional theories*, J. Chem. Phys. 98 (1993), pp. 1372–1377.
[20] C. Lee, W. Yang, and R.G. Parr, *Development of the Colle-Salvetti correlation-energy formula into a functional of the electron density*, Phys Rev. B 37 (1988), p. 785.
[21] J.S. Binkley, J.A. Pople, and W.J. Hehre, *Self-consistent molecular orbital methods. 21. Small split-valence basis sets for first-row elements*, J. Am. Chem. Soc. 102 (1980), pp. 939–947.
[22] M.S. Gordon, J.S. Binkley, J.A. Pople, W.J. Pietro, and W.J. Hehre, *Self-consistent molecular-orbital methods. 22. Small split-valence basis sets for second-row elements*, J. Am. Chem. Soc. 104 (1982), pp. 2797–2803.
[23] W.J. Pietro, M.M. Francl, W.J. Hehre, D.J. DeFrees, J.A. Pople, and J.S. Binkley, *Self-consistent molecular orbital methods. 24. Supplemented small split-valence basis sets for second-row elements*, J. Am. Chem. Soc. 104 (1982), pp. 5039–5048.
[24] P.K. Naik, S. Santoshi, A. Rai, and H.C. Joshi, *Molecular modelling and competition binding study of Br-noscapine and colchicine provide insight into noscapinoid-tubulin binding site*, J. Mol. Graphics Modell. 29 (2011), pp. 947–955.
[25] P.J. Goodford, *A computational procedure for determining energetically favourable binding sites on biologically important macromolecules*, J. Med. Chem. 28 (1985), pp. 849–857.
[26] J. Wang, W. Wang, P.A. Kollman, and D.A. Case, *Automatic atom type and bond type perception in molecular mechanical calculations*, J. Mol. Graphics Modell. 25 (2006), pp. 247–260.
[27] A. Jakalian, D.B. Jack, and C.I. Bayly, *Fast, efficient generation of high-quality atomic charges. AM1-BCC model: II. Parameterization and validation*, J. Comput. Chem. 23 (2002), pp. 1623–1641.
[28] W.L. Jorgensen, J. Chandrasekhar, J.D. Madura, R.W. Impey, and M.L. Klein, *Comparison of simple potential functions for simulating liquid water*, J. Chem. Phys. 79 (1983), pp. 926–935.
[29] T. Darden, D. York, and L. Pedersen, *Particle mesh Ewald: An N log (N) method for Ewald sums in large systems*, J. Chem. Phys. 98 (1993), pp. 10089–10092.
[30] U. Essmann, L. Perera, M.L. Berkowitz, T. Darden, H. Lee, and L.G. Pedersen, *A smooth particle mesh Ewald method*, J. Chem. Phys. 103 (1995), pp. 8577–8593.
[31] J.-P. Ryckaert, G. Ciccotti, and H.J. Berendsen, *Numerical integration of the Cartesian equations of motion of a system with constraints: Molecular dynamics of n-alkanes*, J Comput Phys. 23 (1977), pp. 327–341.
[32] B. Honig and A. Nicholls, *Classical electrostatics in biology and chemistry*, Science 268 (1995), pp. 1144–1144.
[33] I. Massova and P.A. Kollman, *Combined molecular mechanical and continuum solvent approach (MM-PBSA/GBSA) to predict ligand binding*, Perspect. Drug Discovery Des. 18 (2000), pp. 113–135.
[34] A.C. Wallace, R.A. Laskowski, and J.M. Thornton, *LIGPLOT: A program to generate schematic diagrams of protein-ligand interactions*, Protein Eng. 8 (1995), pp. 127–134.